Qingsong ZHOU, Jialong QIAN, Zhongping YANG, et al., 2025. Robust wideband waveform design with constant modulus and discrete phase constraints for distributed precision jamming. *Front Inform Technol Electron Eng*, 26(1):119-133.
https://doi.org/10.1631/FITEE.2400285

Robust wideband waveform design with constant modulus and discrete phase constraints for distributed precision jamming

Key words: Wideband waveform design; Constant modulus (CM); Discrete phase; Riemannian conjugate gradient (RCG); Distributed precision jamming (DPJ)

Corresponding author: Zhongping Yang
E-mail: yangzhongping14@nudt.edu.cn
ORCID: https://orcid.org/0000-0002-5881-0597

Motivation

1. Conventional blanket jamming methods, typically implemented by a single high-power jammer, suffer from low utilization efficiency and can inadvertently affect friendly devices due to their spatial limitations.
2. The introduction of beamforming techniques aims to enhance jamming effectiveness but still poses risks to adjacent friendly devices, highlighting the need for more sophisticated jamming strategies.
3. The existing methods for waveform design face high computational burdens and are not suitable for the minimax multi-objective problem (MOP) inherent in distributed precision jamming (DPJ) scenarios.

Main idea

1. Compared with previous works on the narrowband constant modulus (CM) discrete phase waveform design, we use the wideband signal model to design the CM discrete phase waveform for DPJ.

2. The Riemannian conjugate gradient for CM discrete phase constraints (RCG-CMDPC) algorithm is proposed to address the large-scale optimization problem with CM and discrete phase constraints.

3. The effectiveness of the proposed algorithm is validated through numerical simulations, demonstrating superior jamming efficiency and lower computational demands compared to existing methods.

Problem formulation

1. Signal model

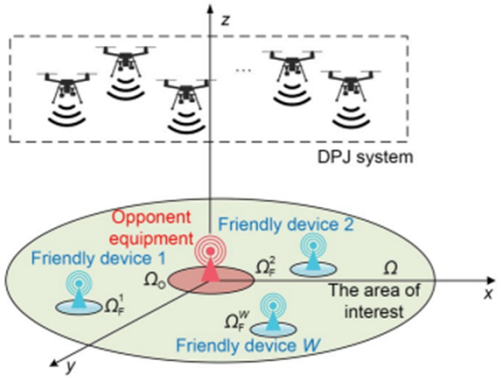

Fig. 1 Blanket jamming action implemented by the distributed precision jamming (DPJ) system consisting of M drones

Therefore, based on Eqs. (1)–(4), the CPS at the spatial frequency point (σ_z, q) is given by Eq. (5):

$$\boldsymbol{P}_{\sigma_z,q}=\left|\boldsymbol{a}_{\sigma_z,q}^{\mathrm{H}}\boldsymbol{y}_q\right|^2=\left|\boldsymbol{a}_{\sigma_z,q}^{\mathrm{H}}\boldsymbol{F}_q\boldsymbol{x}\right|^2=\boldsymbol{x}^{\mathrm{H}}\boldsymbol{\Pi}_{\sigma_z,q}\boldsymbol{x}, \tag{5}$$

where $\boldsymbol{y}_q=\left[y_1(q),y_2(q),\cdots,y_M(q)\right]^{\mathrm{T}}$, $\boldsymbol{F}_q=\left(\boldsymbol{f}_q^{\mathrm{T}}\otimes\boldsymbol{I}_M\right)\in\mathbb{C}^{M\times MN}$, $\boldsymbol{x}=\left[\boldsymbol{x}_1^{\mathrm{T}},\boldsymbol{x}_2^{\mathrm{T}},\cdots,\boldsymbol{x}_M^{\mathrm{T}}\right]^{\mathrm{T}}\in\mathbb{C}^{MN}$, and $\boldsymbol{\Pi}_{\sigma_z,q}=\boldsymbol{F}_q^{\mathrm{H}}\boldsymbol{a}_{\sigma_z,q}\boldsymbol{a}_{\sigma_z,q}^{\mathrm{H}}\boldsymbol{F}_q$ is defined as the steering matrix of the spatial frequency point (σ_z, q).

2. Metric and waveform constraint design

$$\begin{cases} f_1(\boldsymbol{x})=\min\limits_{\sigma_{\mathrm{O}}\in\Omega_{\mathrm{O}},q_{\mathrm{O}}\in\Xi_{\mathrm{O}}}\boldsymbol{x}^{\mathrm{H}}\boldsymbol{\Pi}_{\sigma_{\mathrm{O}},q_{\mathrm{O}}}\boldsymbol{x} \\ \qquad=\max\limits_{\sigma_{\mathrm{O}}\in\Omega_{\mathrm{O}},q_{\mathrm{O}}\in\Xi_{\mathrm{O}}}-\boldsymbol{x}^{\mathrm{H}}\boldsymbol{\Pi}_{\sigma_{\mathrm{O}},q_{\mathrm{O}}}\boldsymbol{x}, \\ f_2(\boldsymbol{x})=\max\limits_{\sigma_{\mathrm{F}}\in\Omega_{\mathrm{F}},q_{\mathrm{F}}\in\Xi_{\mathrm{F}}}\boldsymbol{x}^{\mathrm{H}}\boldsymbol{\Pi}_{\sigma_{\mathrm{F}},q_{\mathrm{F}}}\boldsymbol{x}, \end{cases} \tag{6}$$

where $\Omega_{\mathrm{F}}=\Omega_{\mathrm{F}}^1\cup\Omega_{\mathrm{F}}^2\cup\cdots\cup\Omega_{\mathrm{F}}^W$ is the union of all the W friendly regions, and σ_{O} and σ_{F} represent the discrete spatial points in Ω_{O} and Ω_{F}, respectively. Meanwhile, q_{O} and q_{F} denote the discrete frequency points in the frequency bands Ξ_{O} and Ξ_{F} of opponent and friendly devices, respectively.

3. Optimization problem

Based on the design metrics and waveform constraints, we formulate the minimax MOP as follows:

$$\mathcal{P}\begin{cases} \min\limits_{\boldsymbol{x}}\max\limits_{\sigma_{\mathrm{O}}\in\Omega_{\mathrm{O}},q_{\mathrm{O}}\in\Xi_{\mathrm{O}}}-\boldsymbol{x}^{\mathrm{H}}\boldsymbol{\Pi}_{\sigma_{\mathrm{O}},q_{\mathrm{O}}}\boldsymbol{x} \\ \min\limits_{\boldsymbol{x}}\max\limits_{\sigma_{\mathrm{F}}\in\Omega_{\mathrm{F}},q_{\mathrm{F}}\in\Xi_{\mathrm{F}}}\boldsymbol{x}^{H}\boldsymbol{\Pi}_{\sigma_{\mathrm{F}},q_{\mathrm{F}}}\boldsymbol{x} \\ \text{s.t. } \left|\boldsymbol{x}_i\right|=1,\ i=1,2,\cdots,MN, \\ \qquad \arg(\boldsymbol{x}_i)\in\Psi_V,\ i=1,2,\cdots,MN. \end{cases} \tag{9}$$

Method

To obtain the wideband CM discrete phase waveform for robust DPJ, we propose the RCG-CMDPC algorithm.

1. First, we use L_p approximation and the Pareto optimization framework to transform the original minimax MOP $\mathcal{P}$ into a single-objective minimization problem with CM and discrete phase constraints.

2. Then, the transformed problem is tackled by our proposed RCG-CMDPC algorithm.

3. Finally, we provide the computational complexity analysis of the proposed RCG-CMDPC algorithm.

Algorithm 1 The proposed RCG-CMDPC algorithm for tackling $\tilde{\mathcal{P}}$

Input: Initial point $\boldsymbol{x}^{(0)} \in \mathcal{M}$

Output: The optimal solution $\boldsymbol{x}^{(\mathrm{opt})} \in \mathcal{M}$

Initialize $l=1$

Compute $\boldsymbol{d}^{(0)}=-\mathrm{grad} f_\rho(\boldsymbol{x}^{(0)})$ and the step size $\zeta^{(0)}$

Obtain the intermediate variable $\tilde{\boldsymbol{x}}^{(1)}=\boldsymbol{x}^{(0)}+\zeta^{(0)}\boldsymbol{d}^{(0)}$, and update $\boldsymbol{x}^{(1)}=\Re(\tilde{\boldsymbol{x}}^{(0)})$

Repeat

  Compute the Riemannian gradient $\mathrm{grad} f_\rho(\boldsymbol{x}^{(l)})$ using Eqs. (20) and (21)

  Calculate the Polark–Ribière parameter $\mu^{(l)}$ using Eq. (24)

  Update $\boldsymbol{d}^{(l)}$ and $\mathrm{Trans}\boldsymbol{d}^{(l-1)}$ using Eqs. (22) and (23), respectively

  Compute the step size $\zeta^{(l)}$ by Armijo's back tracking method in Eq. (27)

  Update $\tilde{\boldsymbol{x}}^{(l+1)}=\boldsymbol{x}^{(l)}+\zeta^{(l)}\boldsymbol{d}^{(l)}$

  Implement retraction and update $\boldsymbol{x}^{(l+1)}=\Re(\tilde{\boldsymbol{x}}^{(l+1)})$ using Eq. (26)

  Let $l=l+1$

until $\left|f_\rho(\boldsymbol{x}^{(l+1)})-f_\rho(\boldsymbol{x}^{(l)})\right| / f_\rho(\boldsymbol{x}^{(l)}) \le \varepsilon$, then output $\boldsymbol{x}^{(\mathrm{opt})}=\boldsymbol{x}^{(l)}$

Method

Computational complexity of the proposed RCG-CMDPC algorithm, disregarding the coefficients of high-order terms.

Table 1 Computational complexity summary of the RCG-CMDPC algorithm

Computation	Complexity
$\mathrm{Grad} f_\rho(\boldsymbol{x}^{(l)})$	$O\big((U_{\mathrm{O}}Q_{\mathrm{O}}+U_{\mathrm{F}}Q_{\mathrm{F}})MN + (U_{\mathrm{O}}+U_{\mathrm{F}})M^2N\big)$
$f_\rho(\boldsymbol{x}^{(l)})$	$O\big((U_{\mathrm{O}}Q_{\mathrm{O}}+U_{\mathrm{F}}Q_{\mathrm{F}})MN\big)$
$\mathrm{grad} f_\rho(\boldsymbol{x}^{(l)})$	$O(MN)$
$\mu^{(l)}$	$O(MN)$
$\mathrm{Trans}\boldsymbol{d}^{(l-1)}$	$O(MN)$
$\boldsymbol{d}^{(l)}$	$O(MN)$
$\zeta^{(l)}$	$O(MN)$
$\boldsymbol{x}^{(l+1)}$	$O(MN)$

Major results

Verification of DPJ effectiveness by the CPS distribution, adopting majorization-minimization (MM) and RCG-CMDPC algorithms in typical DPJ scenarios.

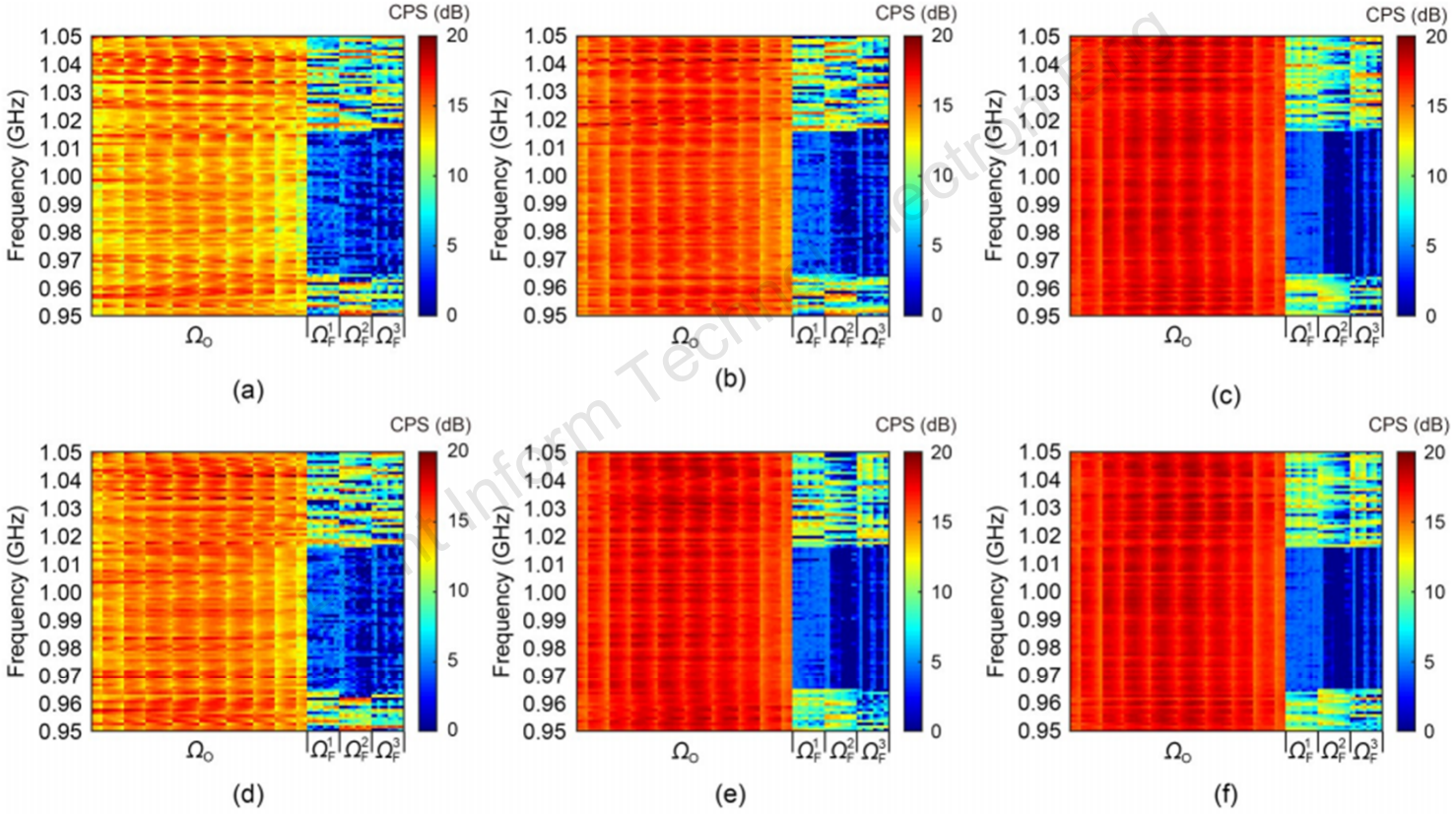

Fig. 3 Combined power spectrum (CPS) distribution in Ω_O and Ω_F with the adoption of different algorithms for case 1: (a) majorization–minimization (MM) algorithm (V=256; discrete phase); (b) MM algorithm (V=1024; discrete phase); (c) MM algorithm (V=∞; continuous phase); (d) Riemannian conjugate gradient for constant modulus discrete phase constraints (RCG-CMDPC) algorithm (V=256; discrete phase); (e) RCG-CMDPC algorithm (V=1024; discrete phase); (f) RCG-CMDPC algorithm (V=∞; continuous phase). References to color refer to the online version of this figure

Major results

Verification of DPJ effectiveness by the CPS distribution, adopting MM and RCG-CMDPC algorithms, where the working frequency of friendly devices is set the same as that of the opponent equipment.

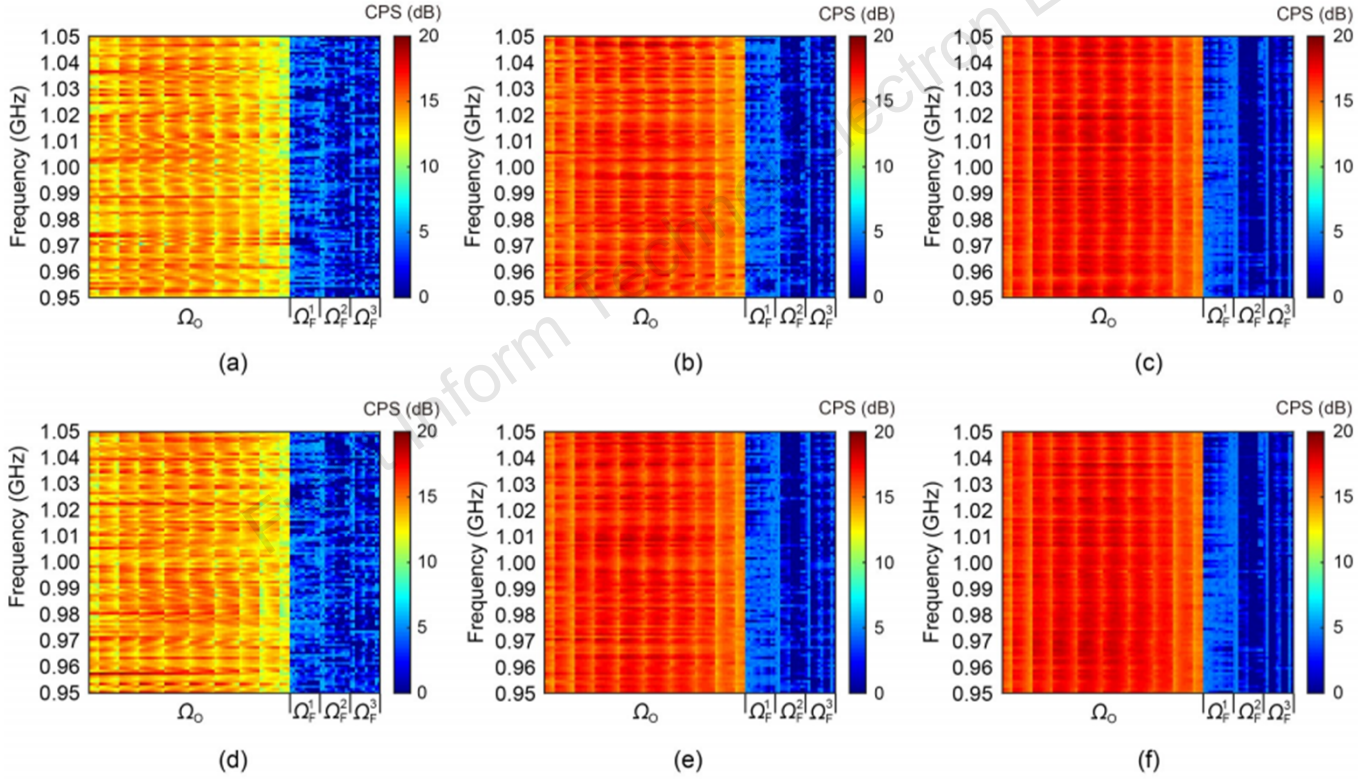

Fig. 4 CPS distribution in Ω_O and Ω_F with the adoption of different algorithms for case 2: (a) MM algorithm (V=256; discrete phase); (b) MM algorithm (V=1024; discrete phase); (c) MM algorithm (V=∞; continuous phase); (d) RCG-CMDPC algorithm (V=256; discrete phase); (e) RCG-CMDPC algorithm (V=1024; discrete phase); (f) RCG-CMDPC algorithm (V=∞; continuous phase). References to color refer to the online version of this figure

Major results

The detailed CPS indicators of these two algorithms are shown in Table 3, where $CPS_O^{\min}$ and CPS_O^{ave} denote the minimum and average $CPSs$ in Ω_O, respectively, while $CPS_F^{\max}$ and CPS_F^{ave} the maximum and average $CPSs$ in Ω_F, respectively.

Table 3 CPS indicators in Ω_O and Ω_F for cases 1 and 2

V	Algorithm	$CPS_O^{\min}$ (dB) (case 1/2)	$CPS_F^{\max}$ (dB) (case 1/2)	CPS_O^{ave} (dB) (case 1/2)	CPS_F^{ave} (dB) (case 1/2)
256 (discrete phase)	MM	8.63/7.87	6.49/6.39	14.37/13.97	3.11/2.91
	RCG-CMDPC	11.20/8.79	6.30/6.29	15.08/14.24	3.02/3.00
1024 (discrete phase)	MM	12.92/12.78	5.68/5.70	15.97/15.93	3.04/2.70
	RCG-CMDPC	14.46/13.64	5.02/5.32	17.01/16.39	2.50/2.55
∞ (continuous phase)	MM	14.85/14.01	4.84/5.18	17.23/16.76	2.31/2.33
	RCG-CMDPC	15.03/14.12	4.82/5.17	17.37/16.81	2.35/2.77

Major results

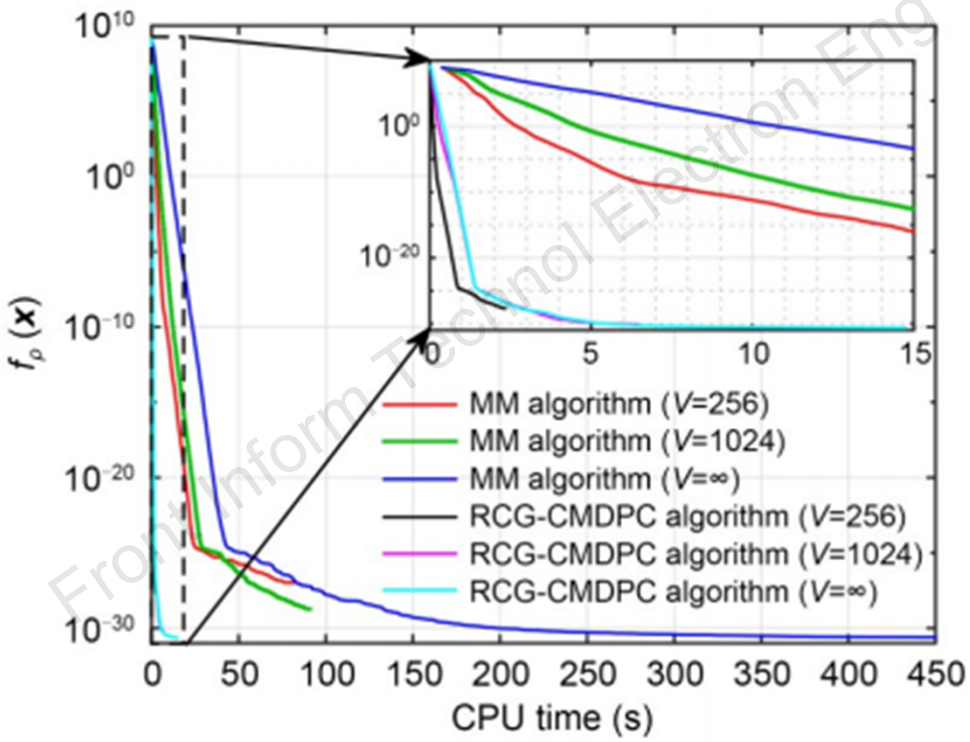

Fig. 5 Convergence curves of the MM and RCG-CMDPC algorithms

Major results

Effect of L_p-norm adoption on the performance of RCG-CMDPC, at $V = 1024$, which means that each jammer is equipped with a 10-bit DDS

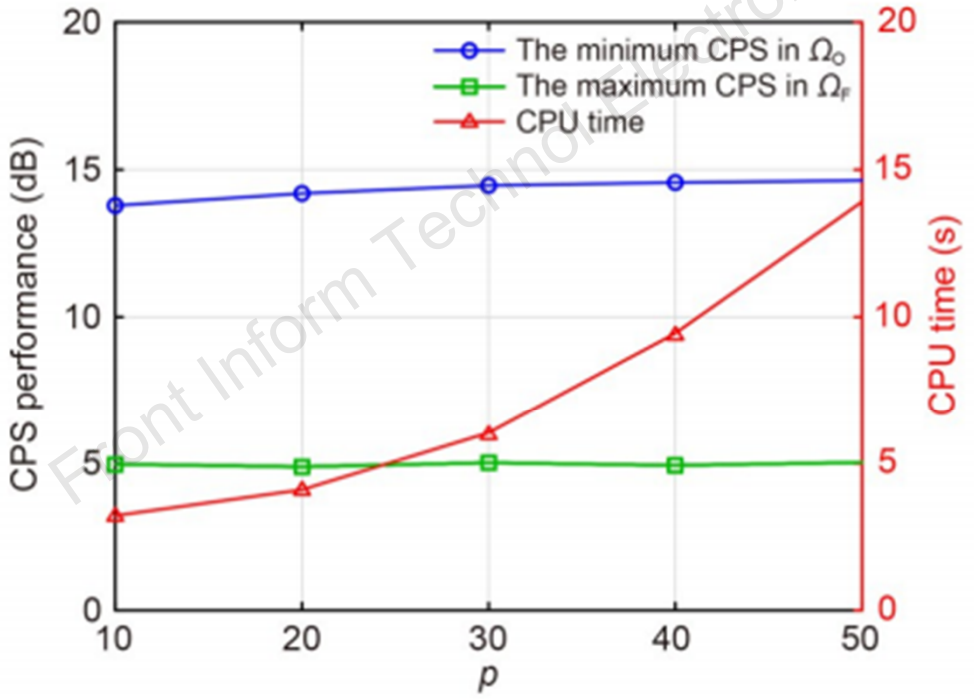

Fig. 6 Effect of value of p on the RCG-CMDPC algorithm performance

Major results

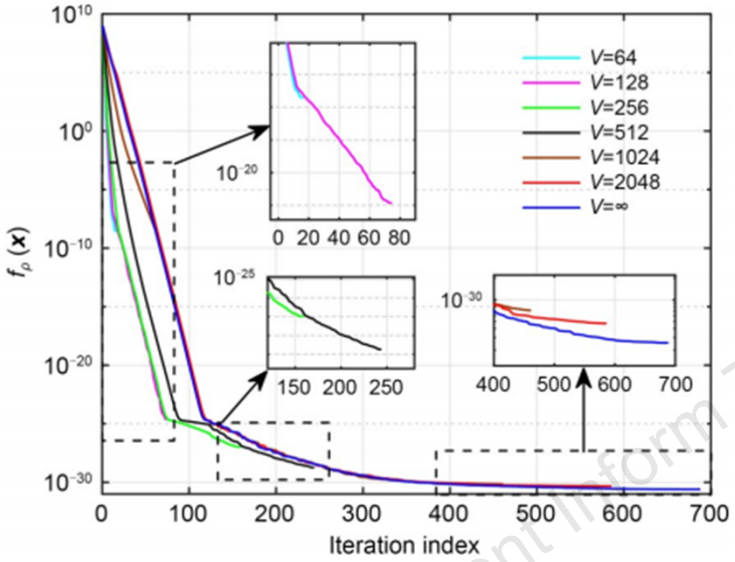

Fig. 7 Variation of $f_\rho(x)$ versus iteration index under different V values

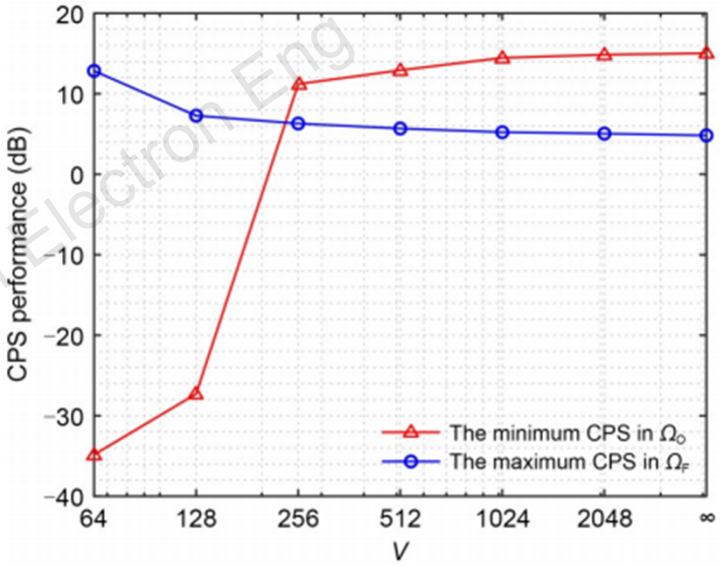

Fig. 8 Effect of V on the CPS performance of the RCG-CMDPC algorithm

Major results

When ρ=1 and 0, the obtained wideband waveform considers only Ω_O and Ω_F, respectively.

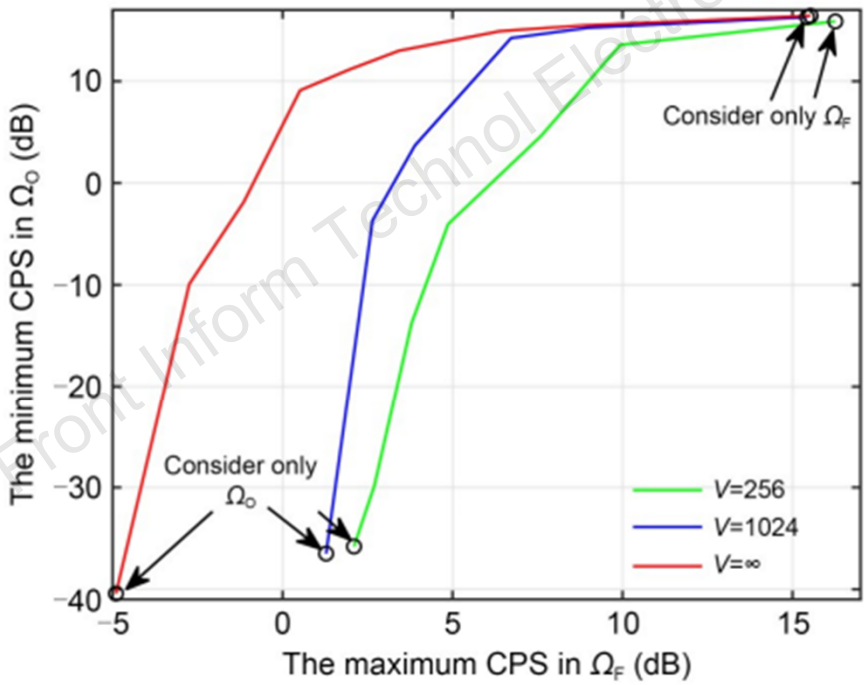

Fig. 9 Performance trade-off between the CPS in Ω_O and Ω_F under different V values

Conclusions

1. We propose an efficient algorithm to design a robust wideband CM discrete phase waveform for DPJ.

2. The corresponding design model is formulated as a minimax MOP, which is transformed as $\mathcal{P}$ using the L_P-norm and Pareto framework.

3. We develop an efficient RCG-CMDPC algorithm within the RCG framework, whereby a novel retraction and projection method is provided to let the solution satisfy the CM discrete phase constraints.

4. The proposed RCG-CMDPC algorithm has lower computational complexity than the competing MM algorithm in theory.

Qingsong Zhou received the M.S. and Ph.D. degrees from the Electronic Engineering Institute, Hefei, China, in 2008 and 2011, respectively. He is currently an Associate Professor with the College of Electronic Engineering, National University of Defense Technology, Hefei, China. His research interests include mainly radar signal processing and convex optimization.

Zhongping Yang received the B.S. and M.S. degrees in information and communication engineering from the National University of Defense Technology, China, in 2018 and 2021, respectively. He is currently working toward the Ph.D. degree with the College of Electronic Engineering, National University of Defense Technology, Hefei, China. His research interests include array signal processing, nonconvex optimization, and electronic warfare.